Reply

KIRSTY HANLEY AND STEPHEN BELCHER

Department of Meteorology, University of Reading, Reading, United Kingdom

PETER SULLIVAN

NCAR, Boulder, Colorado

(Manuscript received and in final form 18 February 2011)

1. Introduction

Hanley et al. (2010, hereafter HBS) present a global climatology of wind–wave interaction based on the inverse wave age $(U_{10}\cos\theta)/c_p$, where U_{10} is the wind speed at a height of 10 m, c_p is the phase speed of the waves at the spectral peak, and θ is the angle between the wind and the direction of propagation of the dominant waves. Their paper examines the extent to which the local wave field is coupled to the local wind field and also seeks to determine which regions of the ocean are in a wind-driven wave regime and which are in a wave-driven wind regime; the latter region is most often dominated by fast-moving swell. The commentary by Högström et al. (2011, hereafter HSSR) argues that, for climatological mapping, the effect of waves on the air–sea momentum exchange should instead be based on the parameter U_{10}/c_p, rather than $(U_{10}\cos\theta)/c_p$. HSSR motivate their commentary with a simple example choosing parameters with $c_p = 12$ m s^{-1}, $U_{10} = 10$ m s^{-1}, and $\theta = 80°$. In this case, $U_{10}/c_p = 0.83$, which implies wind–wave equilibrium (see Csanady 2001), whereas $(U_{10}\cos\theta)/c_p = 0.14$ implies wind–wave disequilibrium with an air–sea momentum flux directed upward from the ocean to the atmosphere. To characterize the above situation as a fully developed sea seems an incorrect diagnosis: the winds and waves are clearly not in equilibrium simply because they are not aligned! The cases of winds parallel and perpendicular to monochromatic wave crests also illustrates the point that U_{10}/c_p would be identical, but $(U_{10}\cos\theta)/c_p$ correctly characterizes the cases as very different. These arguments seem to rule out the use of the parameter U_{10}/c_p as a general wind–wave interaction parameter. The wind–wave interaction parameter $(U_{10}\cos\theta)/c_p$ does however need further motivation, and so here we summarize some of the theoretical support for using $(U_{10}\cos\theta)/c_p$.

2. Wind–wave momentum exchange for a sinusoidal wave

The momentum exchange between the wind and a single monochromatic wave is given by

$$\tau_w = \frac{1}{2}\rho_w \beta a^2 k c \tag{1}$$

where ρ_w is the density of water, a is the wave amplitude, k is the wavenumber, c is the wave phase speed, and β is the wave growth rate parameter.

The dependence on wind–wave angle comes from the wave growth rate β, which describes the rate of growth or decay of a wave spectral component; it is defined (e.g., Belcher and Hunt 1998) as

$$\beta = \frac{1}{E}\frac{\partial E}{\partial t} = c_\beta \omega \frac{\rho_a}{\rho_w}\left(\frac{u_*}{c}\right)^2, \tag{2}$$

where E is wave energy, ω is the wave angular frequency, ρ_a is the density of air, u_* is the friction velocity at the surface, and c_β is the nondimensional wave growth rate coefficient. Calculations by Cohen and Belcher (1999) and Mastenbroek (1996) have shown that, for fast waves with $c/u_* > 20$, c_β is negative (i.e., the waves lose momentum to the wind).

The angular dependence of the wave growth rate has also been investigated. Numerical simulations of turbulent

Corresponding author address: Kirsty Hanley, Department of Meteorology, University of Reading, P.O. Box 243, Reading RG6 6BB, United Kingdom.
E-mail: k.e.hanley@reading.ac.uk

DOI: 10.1175/JPO-D-11-051.1

airflow over 2D waves performed by Li et al. (2000) showed that, for constant values of c/u_*, the wave growth rate varies with θ. Meirink et al. (2003) investigated the dependence of the turbulent airflow over water waves on θ using a semi-analytical model. They found that the wind component in the wave direction largely determines the wave growth rate and that contributions from the transverse wind component are small, even for fast waves. Meirink et al. (2003) show that β collapses when plotted against $(u_* \cos\theta)/c$, which is of course strongly correlated with $(U_{10} \cos\theta)/c$.

Finally, note that the theory is, of course, Galilean invariant and so can be framed in terms of the vector wind speed relative to the wave speed U_{rel}, which, with the wave propagation taken along the x axis, is given by

$$U_{\text{rel}} = U - c = (U\cos\theta - c,\ U\sin\theta). \tag{3}$$

The component perpendicular to the wave is then $(U\cos\theta/c - 1)$, which is a function of only $(U\cos\theta)/c$. Hence, the arguments for the relative angle α between the wind and the moving wave put forward in HSSR are accounted for in this formulation and can be characterized entirely by $(U\cos\theta)/c$.

In conclusion, both the formula for momentum exchange and the growth rate parameter contained within this formula depend on the component of the wind perpendicular to the wave crests. Hence, for a monochromatic wave $(U\cos\theta)/c$ has sound theoretical support.

3. Wind–wave momentum exchange in a spectrum of waves

For a spectrum of waves, following Makin et al. (1995) and Hara and Belcher (2002), the transfer of momentum across the air–sea interface $\boldsymbol{\tau}_w$ is given by the sum of the momentum exchange between the wind and waves summed over all Fourier wave components. Hence, a precise calculation requires the directional spectrum of the waves. This is a difficult calculation to complete in practice for climatological time scales, and so HBS seek to simplify the calculation by characterizing the wave spectrum by a single wave speed and direction c_p. The momentum exchange is then characterized by $(U_{10}\cos\theta)/c_p$. Using this simple parameter, HBS could then compute global statistics using data archived in the 40-yr European Centre for Medium-Range Weather Forecasts (ECMWF) Re-Analysis (ERA-40; Uppala et al. 2005).

In pure wind seas, characterization of the wave spectrum by c_p is common (e.g., Grachev and Fairall 2001). In the case of swell-dominated seas, calculations by Hanley and Belcher (2008) showed that the wave-induced stress is dominated by contributions from the peak in the swell spectrum, again c_p. They showed that the sign of the wave-induced stress is largely determined by $(U_{10}\cos\theta)/c_p$, because this parameter largely distinguishes the part of the swell spectrum that gives up momentum to the wind from the part that takes momentum from the wind. Furthermore, Grachev and Fairall (2001) demonstrate with their ocean observations that the sign reversal of the air–sea momentum flux occurs when $(U_{10}\cos\theta)/c_p$ drops below about 0.15–0.2. They did not find a good collapse of the data when plotted against U_{10}/c_p. Therefore, $(U_{10}\cos\theta)/c_p$ was chosen by HBS as a simple way to obtain a first estimate of the importance of upward momentum transfer from the global ocean.

In mixed seas, where both swell and wind waves are present, the effectiveness of characterizing the spectrum and hence the exchange of momentum between wind and waves by a single wave speed c_p is problematic. Instead, the momentum flux should be calculated as a Fourier sum over the entire wave spectrum. The division of the wave spectrum into two parts, a swell component and a wind sea component, as suggested by HSSR, may be a useful approximation. Nevertheless, the arguments here suggest that the simple method used by HBS should characterize the extremes of pure swell and pure wind sea, which appears to be their objective.

4. Global perspective

One of the main conclusions of HBS was that purely wind-driven seas occur most frequently in the midlatitude storm tracks and that upward momentum transfer is most likely to occur in the tropical eastern ocean basins. To determine how the definition of inverse wave age would affect this result, we have computed global maps of $(U_{10}\cos\theta)/c_p$ and U_{10}/c_p averaged over a single year, 1990 (see Fig. 1). Figure 1a, which used $(U_{10}\cos\theta)/c_p$, is in good agreement with the 44-yr climatology of $(U_{10}\cos\theta)/c_p$ computed in Fig. 6 of HBS. This indicates that data from 1990 is representative of the 44-yr climatology.

The overall patterns obtained using $(U_{10}\cos\theta)/c_p$ and U_{10}/c_p are similar, but the patterns are blurred in Fig. 1b when compared to Fig. 1a. The highest values of inverse wave age occur in the midlatitude storm tracks and the lowest values in the tropics. The climatology of $(U_{10}\cos\theta)/c_p$ identifies the tropical eastern ocean basins, just off the coasts of Indonesia, Southern California, South America, and Africa, as the regions where upward momentum transfer would be most likely. In these regions, wind speeds are typically low and generally easterly in direction, whereas fast-moving swell is propagating northward out of the Southern Ocean. This leads to large values of θ, and as a result the climatology of U_{10}/c_p

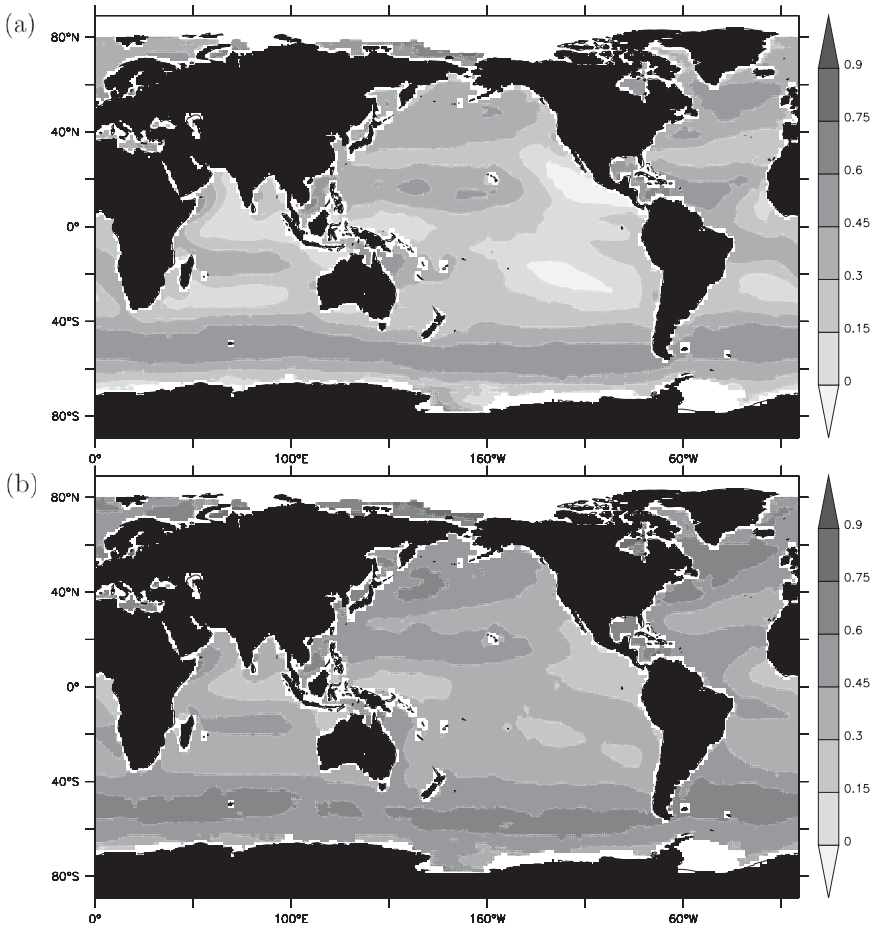

FIG. 1. Inverse wave age calculated using the ERA-40 data averaged over 1990 computed as (a) $(U_{10}\cos\theta)/c_p$ and (b) U_{10}/c_p.

gives higher values in these regions than the climatology of $(U_{10}\cos\theta)/c_p$. However, the lowest values of U_{10}/c_p are also found in these regions: there are large areas where $U_{10}/c_p < 0.3$. Therefore, both maps suggest that the tropical eastern ocean basins are the regions of the global ocean where upward momentum transfer is most likely to occur.

The inverse wave age is also a useful indicator of the degree of wind–wave coupling: high values of inverse wave age indicate regions where the waves are strongly coupled to the local wind field and low values indicate regions where nonlocal wave components (i.e., swell) are present. The climatologies in HBS show that the wind–wave coupling is strongest in the midlatitude storm tracks and weakest in the tropics. The fully developed limit for waves forced by the local wind is reached when $U_{10}/c_p = 0.83$. In HBS, no regions were identified where the inverse wave age is greater than 0.83, which suggests that remotely generated swell is generally present everywhere in the global ocean. This result is robust to both definitions of the inverse wave age: neither plot in Fig. 1 shows regions of the ocean where the wind speed exceeds the wave speed, even in the midlatitude storm tracks. Including the $\cos\theta$ term reduces the magnitude of the inverse wave age everywhere, indicating that the fully developed state of wind–wave alignment is very rare in the global ocean. This is further evidence that remotely generated swell is generally present in the global ocean and that the local wind and wave fields are rarely in equilibrium. We conclude that the main results reported in HBS do not depend critically on the definition of the wave age parameter.

5. Conclusions

HSSR suggested that, for global mapping of the air–sea momentum exchange using the inverse wave age, the parameter U_{10}/c_p should be used. Because the wave growth rate is determined mainly by the wind in the wave direction, the momentum flux varies as the angle between the wind and the waves varies; therefore, we

have argued that $(U_{10}\cos\theta)/c_p$ is a better parameter to use. We have shown here that the main conclusions from HBS—(i) that the local wind and waves are often in a state of nonequilibrium with remotely generated swell generally present, (ii) that the waves are most strongly coupled to the local wind in the midlatitude storm tracks and (iii) that upward momentum transfer is most likely to occur in the tropical eastern ocean basins—are robust to the definition chosen for the inverse wave age.

Finally we note that, as discussed in section 3, a more precise climatology would require calculation of the exchange of momentum between the wind and waves by integrating over the entire wave spectrum. It might be that separating the wave spectrum into two parts, one characterizing the swell and another characterizing the wind sea, as suggested by HSSR, provides a useful simplification. However, the effectiveness of this simplification remains to be demonstrated. It seems likely that more precise calculations of the momentum exchange will enable better interpretation of the specific case studies, such as those presented in HSSR.

REFERENCES

Belcher, S. E., and J. C. R. Hunt, 1998: Turbulent flow over hills and waves. *Annu. Rev. Fluid Mech.,* **30,** 507–538.

Cohen, J. E., and S. E. Belcher, 1999: Turbulent shear flow over fast-moving waves. *J. Fluid Mech.,* **386,** 345–371.

Csanady, G. T., 2001: *Air-Sea Interaction: Laws and Mechanisms*. Cambridge University Press, 239 pp.

Grachev, A. A., and C. W. Fairall, 2001: Upward momentum transfer in the marine boundary layer. *J. Phys. Oceanogr.,* **31,** 1698–1711.

Hanley, K. E., and S. E. Belcher, 2008: Wave-driven wind jets in the marine atmospheric boundary layer. *J. Atmos. Sci.,* **65,** 2646–2660.

——, ——, and P. P. Sullivan, 2010: A global climatology of wind–wave interaction. *J. Phys. Oceanogr.,* **40,** 1263–1282.

Hara, T., and S. E. Belcher, 2002: Wind forcing in the equilibrium range of wind-wave spectra. *J. Fluid Mech.,* **470,** 223–245.

Högström, U., A.-S. Smedman, A. Semedo, and A. Rutgersson, 2011: Comments on ''A global climatology of wind–wave interaction.'' *J. Phys. Oceanogr.,* **41,** 1811–1813.

Li, P. Y., D. Xu, and P. A. Taylor, 2000: Numerical modelling of turbulent airflow over water waves. *Bound.-Layer Meteor.,* **73,** 159–182.

Makin, V. K., V. N. Kudryavtsev, and C. Mastenbroek, 1995: Drag of the sea surface. *Bound.-Layer Meteor.,* **106,** 171–183.

Mastenbroek, C., 1996: Wind-wave interaction. Ph.D thesis, Delft Technical University, 118 pp.

Meirink, J. F., V. K. Makin, and V. N. Kudryavtsev, 2003: Note on the growth of water waves propagating at an arbitrary angle to the wind. *Bound.-Layer Meteor.,* **106,** 171–183.

Uppala, S. M., and Coauthors, 2005: The ERA-40 Re-Analysis. *Quart. J. Roy. Meteor. Soc.,* **131,** 2961–3012.